INTERNATIONAL JOURNAL OF MULTIDISCIPLINARY EDUCATIONAL RESEARCH
ISSN : 2277-7881
VOLUME 1, ISSUE 4, SEPT 2012

STATIC STRENGTH ANALYSIS OF ELLIPTICAL CHORD TUBULAR T-JOINTS USING FEA

K.S.Narayana
Department of Mechanical Engg.
ANITS
Visakhapatnam

R.T.Naik
Department of Mechanical Engg.
Indian Institute of Science, Bangalore

R.C.Mouli
Department of Mechanical Engg.
ANITS
Visakhapatnam

M.Prasant Kumar
Department of Mechanical Engg.
ANITS
Visakhapatnam

R.T.Babu Naik
National Geophysical Research Institute,
Uppal Road,
Hyderabad

1. INTRODUCTION

1.1 Offshore Structures: Offshore structures used for oil and gas extraction have the common function of providing a safe, dry working environment for the equipment and persons those operates the platform. Jacket supported drilling equipment as a guide for the piled foundations. The substructure referred to as the jacket is a three dimensional space frame made from large tubular steel members. The jacket which takes the loadings from the top side and the sea environment is piled to the sea bed.theses piles must also be able to resist tension as hydrodynamic forces on the structure have a tendency to cause over turning. To construct a steel jacket it is necessary to join the large diameter tubular steel members in somewhere. These tubular joints or nodes are major sources of difficulty and high cost in the design of jacket. Tubular joints can be classified in to four categories. They are the simple welded joints, complex welded joints, cast steel joints and composite joints.

Simple welded joints are those formed by welding two or more tubular members in a single plane without overlapping of brace members and without the use of gussets, diaphragms, stiffeners or grout. Unlike a pipe joint, the chord wall is left intact with the hidden plug regions enclosed by the braces. The geometric and other notation for a simple joint is shown [10] in Figure 1.1

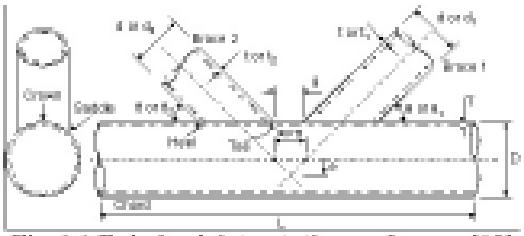

Fig. 1.1 Tubular joint notations reference [10]

1.2 ***Literature review.*** Bolt H.M.et.al [1] described the influence of chord length and boundary conditions on K joint strength.Chen, W. F et.al. [2] Designed the Tubular Members in Offshore structure. Fabricated and shown the merit of cylindrical steel tubular section compared to other sections. Chen & WU [3] used shell elements to model the elastic plastic behavior of T joints with small deflection. Dutt D.et.al, [4] parameters influencing the stress concentration factor join in offshore structures. He explored various configurations in SCF and Loading types. J.S. Jubran and W.F.Cofer [5] who employed the solid elements to generate T joint model. This is found to be successful for evaluating the ultimate joint load. Hameed. A.F. et.al [6] conducted more experimental tests on the Elliptical T-tubular joints, which were compared with circular chord tubular joints. employed shell elements to tackle the stress analysis problem of T tubular joints. The results were compared with experimental data. The experimental approach to obtain the joint data is expensive. The finite element method is found to be a suitable alternative for solving tubular joint . Kanatani [7] carried out some experimental studies on welded tubular connections with different loading cases. But this was limited to only circular tubular joints. Nazari, A.e.al.[8] designed Parametric Study of Hot Spot Stresses Around Tubular Joints With Double Plates. He explained the stress factor concentration at various pipe joints. Strub. D et.al.[9] , Risk Based Acceptance Criteria for Joints Subject to Fatigue Deterioration. He explained the how the joints subjected under fatigue conditions and stress concentrations.Thandavamoorthy T. S.[10] developed the Finite Element Modeling of the Behavior of Internally Ring Stiffened T-Joint of Offshore Platform. He studied the three types of angular rings behavior and their strength under axial compression loading.

2. MODELING OF TUBULAR T-JOINT

2.1 ***Geometric model of the T-joint***: The geometry and the dimensions of the T-joint under study are same as those subjected to experimental investigation by Hameed et al [6] as given in Table 2.1 For the purpose of comparison of experimental results we have taken similar Dimensions in this investigation .The material used in all cases are mild steel. Type-1 refers to brace joined perpendicular to the minor diameter of elliptical chord and Type-2 refers to brace joined perpendicular to the major diameter of elliptical chord.

Table 2.1 Geometric Parameters of the Modeled T-joint for Type-1&Type-2

Geometric Parameter	Chord (mm) Elliptical pipe	Brace (mm) Circular pipe
Minor diameter	60	42.5
Major diameter	90	
Length	440.0	200.0
Thickness	2.0	2.0

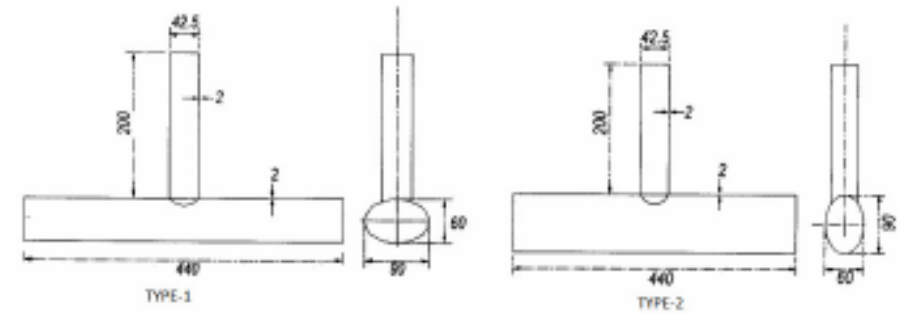

Fig.2.1 Geometry of the models (all dimensions are in mm)

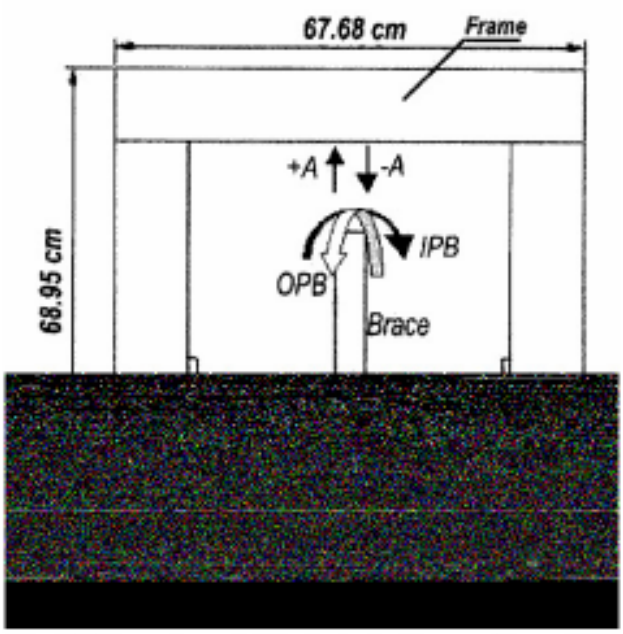

Fig.2.2 Experimental test rig (reference from [6])

2.2 *Boundary conditions*: In experimental study, the chord ends are bolted. The Boundary conditions applied to the chord member of the T-joints are approximated to chord end fixity for all degrees of freedom.

2.3 *Loading conditions*: The chord is held as fixed –fixed from both ends. Detailed weld fillets are not modeled. The loads are applied for all the types to the free end of the brace in different directions, depending on the load type. For tension and compression loading, the loads are uniformly distributed at every node of the free end of the brace, where the upward is for tension loading and downward for compression loading. For IPB loading and OPB loading, the loads are applied to two points at the free end of the brace, where the distance between the two points is the brace diameter d. The load applied at the two points will create a couple (moment) at the free end of the brace and cause the brace to deflect on one side, depending on the way the load is applied. For IPB, the direction of deflection will be parallel to the chord tube while for OPB the direction of deflection will be perpendicular to the chord tube. Only elastic analysis was carried out.

a) Axial tension:

In the axial tension case the load was taken as upward direction is positive. After creating the models [Type-1, Type-2] the chord Tube has to be fixed on both ends. Then the brace has to consider as free end. At the top of the brace the loads applied gradually then the deflection at the Tubular joint was displayed like that we have to do number of other loading cases and observed the displacements then at the maximum deflection the tubular joint was broken and the minimum displacement the tubular joint values are observed. The safe load was obtained at the yield point from the graph which is drawn between applied load and deflection. In this loading case failures occurred at chord position near the joint region where the yielding of the chord appears to occur around the brace.

b) Axial compression:

In the axial compression the downward direction is the load was considered as negative. Basically the same above procedure followed for these loading cases except the load-applied direction was downward. In this analysis also the loads applied at the end of the brace and displacements, stresses, were obtained and tabulated. The maximum yield point obtained by drawing curve between applied loads and

displacements. Similar procedure followed for other tubular joints also. The failure associated with buckling and plastic deformation of the chord wall at brace chord interception.

c) In-plane –bending:

In this case also the chord ends are fixed and brace end was considered as free end. But in bending (the moments) at the end of the brace two points are selected for load application. The distances between two points are equal to the brace diameter. The load also applied parallel to the chord. While applying the load the couple [moment] formed and it deflects parallel to the chord then the displacement stresses were tabulated for the type1, typ2 respectively. The maximum yield point obtained from the graph which is drawn between applied moments and deflection. Failure occurs as the results of fracture of chord wall on tension side of the brace and plastic bending and buckling of the chord on compression side.

d) Out-plane-bending:

In this case also the similar procedure of above case followed except the direction of load application. Here the loads applied at the end of the brace of the two points. The couple formed then the displacements, stresses are tabulated. But in this case the loads are applied perpendicular to the chord Tube. The same procedure followed at different loads for other types of models. The maximum yield point obtained from the graph. In this case the failure occurs as a result of local buckling of the chord wall in the 'vicinity' of the brace saddle and compression side occurs.

2.4 Equations in Static Analysis

After using a discretization scheme to model the continuum, we have obtained an expression for the total potential energy in the body as

$$P= \tfrac{1}{2} Q^T KQ - Q^T F \qquad \textbf{(2.1)}$$

Where K is the structural stiffness matrix, F is the global load vector, and Q is the global displacement vector. Here, K and F are assembled from element stiffness and force matrices, respectively. We now have to arrive at the equations of equilibrium, from which we can determine nodal displacements, element stresses, and support reactions.

The minimum potential energy theorem is now invoked. This theorem is stated as follows: Of all possible displacements that satisfy the boundary conditions of a structural system, those corresponding to equilibrium configurations make the total potential energy to a minimum value. Consequently, the equations of equilibrium can be obtained by minimizing potential energy (P) with respect to Q, the potential energy $P = \frac{1}{2} Q^T KQ - Q^T F$ subject to boundary conditions. Boundary conditions are usually of the type.

$$Q_{p1} = a_1,\ Q_{P2} = a_2,\ Q_{pr} = a_r \qquad \textbf{(2.2)}$$

That is, the displacements along degrees of freedom (d o f) $p_1, p_2, \ldots p_r$ are specified to be equal to $a_1, a_2, \ldots, a_r$, respectively. In other words, there are number of supports in the structure, with each support node given a specified displacement. Generally the term d o f is used here instead of node, since a two-dimensional stress problem will have two degrees of freedom per node.

It should be emphasized that improper specification of boundary conditions can lead to erroneous results. Boundary conditions eliminate the possibility of the structure moving as a rigid body. Further, boundary conditions should accurately model the physical system. Elimination approach for handling specified displacement boundary conditions is give below.

There are multi-point constraints of the type

$$b_1 Q_{p1} + b_2 Q_{p2} = b_0$$

Where b_0, b_1, and b_2 are known constants. These types of boundary conditions are used in modeling inclined roller supports, rigid connections or shrink fits. It should be emphasized that improper specification of boundary conditions can lead to erroneous results. Boundary conditions eliminate the possibility of the structure moving as a rigid body. Further, boundary conditions should accurately model the physical system. Two approaches will now be discussed for handling specified displacement boundary conditions of the type given in Eq.2.1 the elimination approach and the penalty approach. For multi-point constraints in above equation, only the penalty approach will be given, because it is simpler to implement.

To illustrate the basic idea, consider the single boundary condition $Q_1 = a_1$. The equilibrium equation are obtained by minimizing P with respect

To Q, subject to the boundary condition $Q_1 = a_1$. For an N – d o f structure, we have

$$Q = [Q_1, Q_2, Q_N]^T$$

$$F = [F_1, F_2, F_N]^T$$

The global stiffness matrix is of the form

$$K = \begin{bmatrix} K_{11} & K_{12} & \cdots & K_{1N} \\ K_{21} & K_{22} & \cdots & K_{2N} \\ \cdot & & & \\ \cdot & & & \\ K_{N1} & K_{N2} & \cdots & K_{NN} \end{bmatrix}_{N \times N}$$

Note that K is a symmetric matrix. The potential energy $\Pi = \frac{1}{2} Q^T KQ - Q^T F$ can be written in expanded form as:

$$\Pi = \tfrac{1}{2} (Q_1 K_{11} Q_1 + Q1 K_{12} Q_2 + \ldots + Q_1 K_{1N} Q_N + Q_2 K_{21} Q_1 + Q2 K_{22} Q_2 + \ldots + Q_2 K_{2N} Q_N + Q_N K_{N1} Q_1 + QN K_{N2} Q_2 + \ldots + Q_N K_{NN} Q_N - (Q_1 F_1 + Q_2 F_2 + \ldots + QN F_N)$$

If we now substitute the boundary condition $Q_1 = a_1$ into the expression

ForΠ above, we obtain.

$$\Pi = \tfrac{1}{2} (a_1 K_{11} a_1 + a1 K_{12} Q_2 + \ldots + a_1 K_{1N} Q_N + Q_2 K_{21} a_1 + Q2 K_{22} Q_2 + \ldots + Q_2 K_{2N} Q_N + Q_N K_{N1} a_1 + QN K_{N2} Q_2 + \ldots + Q_N K_{NN} Q_N - (a_1 F_1 + Q_2 F_2 + \ldots + Q_N F_N) \quad (2.3)$$

Note that K is a symmetric matrix. The potential energy $\Pi = \frac{1}{2} Q^T KQ - Q^T F$ can be written in expanded form as:

$$\Pi = \tfrac{1}{2} (Q_1 K_{11} Q_1 + Q1 K_{12} Q_2 + \ldots + Q_1 K_{1N} Q_N + Q_2 K_{21} Q_1 + Q2 K_{22} Q_2 + \ldots + Q_2 K_{2N} Q_N + Q_N K_{N1} Q_1 + QN K_{N2} Q_2 + \ldots + Q_N K_{NN} Q_N - (Q_1 F_1 + Q_2 F_2 + \ldots + QN F_N)$$

If we now substitute the boundary condition $Q_1 = a_1$ into the expression

ForΠ above, we obtain.

$$\Pi = \tfrac{1}{2}(a_1 K_{11}a_1 + a1\, K_{12} Q_2 + \ldots + a_1 K_{1N} Q_N + Q_2 K_{21}a_1 + Q2\, K_{22}\, Q_2 + \ldots + Q_2 K_{2N} Q_N + Q_N K_{N1}a_1 + QN\, K_{N2}\, Q_2 + \ldots + Q_N K_{NN} Q_N) - (a_1 F_1 + Q_2 F_2 + \ldots + Q_N F_N) \quad (2.3)$$

Note that the displacement Q_1 has been eliminated in the potential energy expression above. Consequently, the requirement that Π take on a minimum value implies that

$$\frac{d\Pi}{dQ} = 0 \qquad i = 23\ldots\ldots N \quad (2.4)$$

We thus obtain,

$$\begin{aligned} K_{22}Q_2 + K_{23}Q_3 + \ldots + K_{2N}Q_N &= F_2 - K_{21}a_1 \\ K_{32}Q_2 + K_{33}Q_3 + \ldots + K_{3N}Q_N &= F_3 - K_{31}a_1 \\ K_{N2}Q_2 + K_{N3}Q_3 + \ldots + K_{NN}Q_N &= F_N - K_{N1}a_1 \end{aligned} \quad (2.5)$$

The above finite element equations can be expressed in matrix form as

$$\begin{bmatrix} K_{22} & K_{23} & \ldots & K_{2N} \\ K_{32} & K_{33} & \ldots & K_{3N} \\ \cdot & & & \\ \cdot & & & \\ \cdot & & & \\ K_{N2} & K_{N3} & \ldots & K_{NN} \end{bmatrix} \begin{Bmatrix} Q_2 \\ Q_3 \\ \cdot \\ \cdot \\ \cdot \\ Q_N \end{Bmatrix} = \begin{Bmatrix} F_2 - K_{21}a_1 \\ F_3 - K_{31}a_1 \\ \cdot \\ \cdot \\ \cdot \\ F_N - K_{N1}a_1 \end{Bmatrix} \quad (2.6)$$

We now observe that the (N-1 x N-1) stiffness matrix above is obtained simply by deleting or eliminating the first row and column (in view of $Q_1 = a_1$) from the original (N x N) stiffness matrix. Equation 2.6 may be denoted as

$$KQ = F \quad \textbf{(2.7)}$$

Where K above is a reduced stiffness matrix obtained by eliminating the row and column corresponding to the specified or 'support' d o f. Equations 2.7 can be solved for the displacement vector Q using Gaussian elimination. Note that the reduced K matrix is nonsingular, provided the boundary conditions have been specified properly; the original K matrix, on the other hand, is a singular

Matrix . Once Q has been determined, the element stress can be evaluated using the following equation

$$s = EBQ \quad \textbf{(2.8)}$$

Where Q for each element is extracted from Q using element connectivity information.

Assume that displacements and stresses have been determined. It is now necessary to calculate the reaction force R_1 at the support. This reaction force can be obtained from the finite element equation (or equilibrium equation) for node 1:

$$K_{11} Q_1 + K_{12} Q_2 + \ldots + K_{1N} Q_N = F_1 + R_1 \quad \textbf{(2.9)}$$

Here, Q_1, Q_2….. Q_n are known. F_1, which equals the load applied at the support (if any), is also known. Consequently, the reaction force at the node that maintains equilibrium, is

$$R_1 = K_{11} Q_1 + K_{12} Q_2 + \ldots + K_{1N} Q_N - F_1 \quad \textbf{(2.10)}$$

Note that the element K_{11}, K_{12},…K_{1N} used above, which form the first row of K, need to be stored separately. This is because K in Eq. 2.7 is obtained by deleting this row and column from the original K.

The modification to K and F discussed above are also derivable using Galerkin'svariational formulation.

$$Y^T (KQ - F) = 0 \quad \textbf{(2.11)}$$

For every Y consistent with the boundary conditions of the problem. Specifically, consider the constraint

$$Q_1 = a_1 \quad \textbf{(2.12)}$$

Then, we require

$$Y_1 = 0 \quad \textbf{(2.13)}$$

Choosing virtual displacements $Y = [0,1,0,\ldots 0]$, $Y = [0,0,1,0,\ldots 0]^T$, …..

$Y= [0,0,\ldots 0,1]^T$, and substituting each of these into Eq.3.11, we obtain precisely the equilibrium equations given in Eq.2.6.

2.5. Von Mises Stress

Von Mises stress is used as a criterion in determining the onset of failure in ductile materials. The failure criterion states that the Von Mises stress s_{VM} should be less than the yield stress, s_Y of the material. In the inequality form, the criterion may be put as

$$s_{VM} £ s_Y \quad \textbf{(2.14)}$$

The Von Mises stress σ_{VM} is given by

$$\sigma_{VM} = \sqrt{I_1^2 - 3I_2} \qquad (2.15)$$

Where I_1 and I_2 are the first two invariants of the stress tensor. For the general state of stress I_1 and I_2 are given by

$$I_1 = \sigma_x + \sigma_y + \sigma_z$$
$$I_2 = \sigma_x\sigma_y + \sigma_y\sigma_x + \sigma_z\sigma_x - \tau^2_{yz} - \tau^2_{xz} - \tau^2_{xy} \qquad (2.16)$$

In terms of the principal stress σ_1, σ_2, and σ_3 the two invariants can be written as

$$I_1 = \sigma_1 + \sigma_2 + \sigma_3$$
$$I_2 = \sigma_1\sigma_2 + \sigma_2\sigma_3 + \sigma_3\sigma_1 \qquad (2.17)$$

Von Mises stress can be expressed in the form

$$\sigma_{VM} = \frac{1}{\sqrt{2}}\sqrt{(\sigma_1 - \sigma_2)^2 + (\sigma_2 - \sigma_3)^2 + (\sigma_3 - \sigma_{31})^2} \qquad (2.18)$$

2.7. THEORETICAL ANALYSIS

The portion of the chord that is located directly under the brace acts as a significant area as it carries the maximum loads acting on it on both horizontal diametric ends. The displacement distributions can be translated in to approximate load distributions on both chord ends as shown in Figure (2.3) and Figure (2.4).

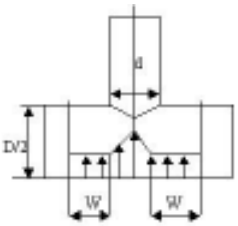

Figure 2.3: Approximate load distribution on compression end of chord

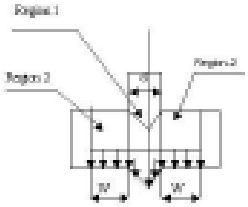

Figure 2.4: Approximate load on Tension end of tension end of chord

3. RESULTS

The results from this work are presented in finite element outputs, followed by final comparison. The result of finite element analysis for an elastic analysis is presented. The Von Misses Stress was obtained for each loading mode and then takes further yield point to serve as a base for comparison. The finite element model of the T-joint, created using ANSYS pre-processor is shown in Figure 3.1.

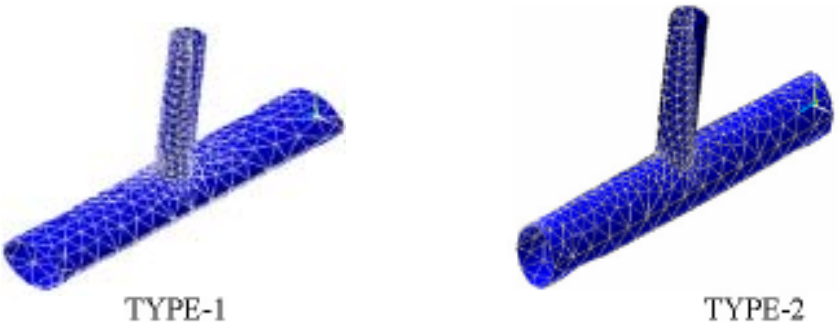

Fig. 3.1: Finite element model of the Tubular T-joint

ANSYS FINITE ELEMENT RESULTS COMPRESSION LOADING FOR TYPE – 1

The meshed model of the T-joint, when subjected to axial compressive load, revealed that the portion of the chord directly under the brace is subjected to high stresses. Von Mises equivalent stress is taken to define yield point. The joint yielded at a compressive load of **25KN**. The displacement distribution on the chord at yield is shown in Figure 3.2. Near the intersection of the members, the displacements are found to be high. As expected the displacements are greatest at the intersection of the branch and chord.

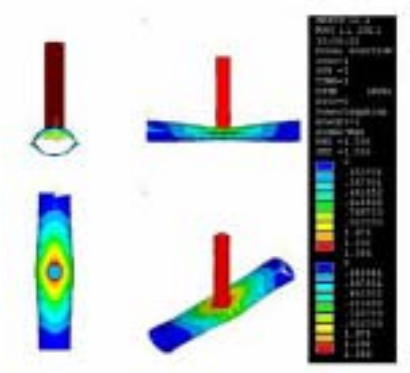

3.2: Finite element model of the Tubular T-joint type - 1

ANSYS FINITE ELEMENT RESULTS OF IN-PLANE BENDING LOADING FOR TYPE – 2

Under in-plane bending moment load, the portion of the chord adjacent to the intersection of the members yielded. The Von Mises stresses are found to equal the yield stress at a bending moment load of **0.75 KN-m**. The displacement distribution

is shown in Figure 3.3. It is observed that one side of the brace acts as tension side and other side as compressive side, with the portion of the cord directly under the brace acts as translational stage between the two sides

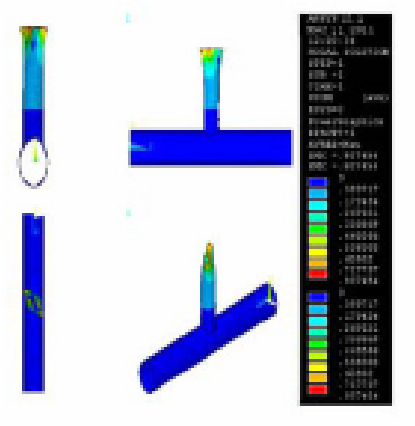

Fig. 3.3: Finite element model of the Tubular T-joint type - 2

ANSYS FINITE ELEMENT RESULTS OF OUT-OF- PLANE BENDING FOR TYPE -2

Under out-of-plane bending moment load, the portion of the chord directly under the brace is found to yield at a load of **0.46 KN-m**, are shown in Figure 3.4

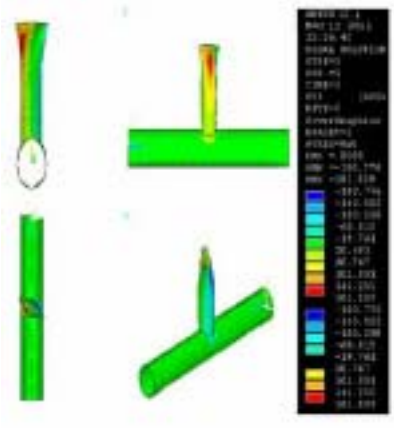

Fig. 3.4: Finite element model of the Tubular T-joint type - 1

Table 3.1 Comparison between Experimental and Finite element results for Tubular T-joint for TYPE-1 (Experiments by Hameed et al [6])

Loading case	Yielding point (FEA) (ANSYS)	Yielding point (Experiment)
Tension (KN)	25.00	24.44
Compression (KN)	25.00	19.40
In-Plane bending (KN-m)	0.55	0.45
Out-of-Plane bending (KN-m)	0.50	0.37

Table 3.2 Comparison between the ANSYS and LUSAS [6] Finite element analysis results for TYPE-1

Loading case	**Yeilding Point (LUSAS)**	**Yeilding Point (ANSYS)**
Tension (kN)	25	25
Compression (kN)	25	25
In-Plane Bending (kN-m)	0.56	0.55
Out-Plane Bending (kN-m)	0.49	0.50

Table 3.3 Comparison between Experimental and Finite element results for Tubular T-joint for TYPE-2 (Experiments by Hameed et al [6])

Loading case	Yielding point (FEA) (ANSYS)	Yielding point (Experiment)	% Error
Tension (KN)	32	31.48	1.625
Compression (KN)	32	29.63	7.40
In-Plane bending (KN-m)	0.75	0.81	8.0
Out-of-Plane bending (KN-m)	0.46	0.48	4.347

Table 3.4 Comparison between the ANSYS and LUSAS [6] Finite element analysis results for TYPE-2

Loading case	Yielding Point (LUSAS)	Yielding Point (ANSYS)
Tension (KN)	32	32
Compression (KN)	32	32
In-Plane Bending (KN-m)	0.75	0.75
Out-Plane Bending (KN-m)	0.47	0.46

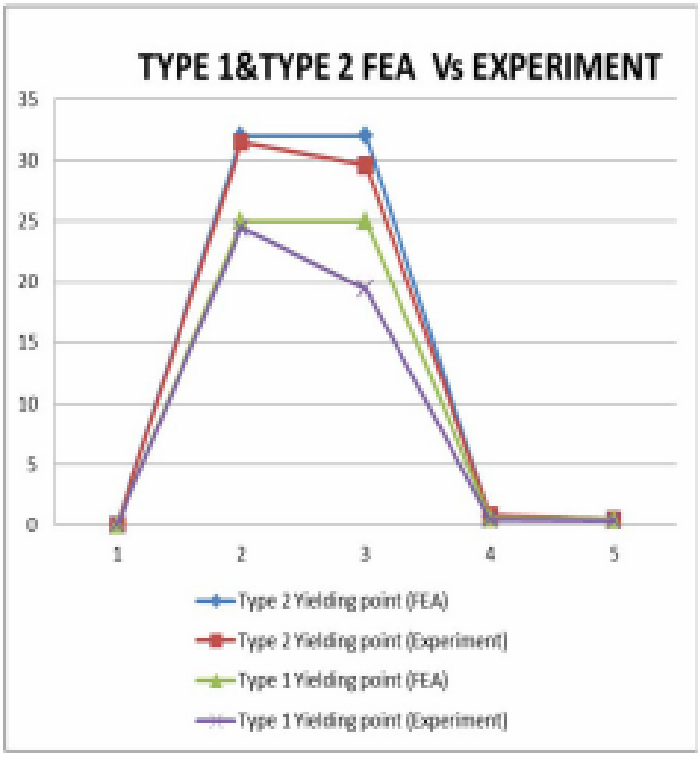

Fig 3.5 Graphical comparison of Type-1 and Type-2. FEA Vs. Experiment.

4. CONCLUSIONS

An elastic analysis has been carried out. The result shows that the circular brace is joined perpendicular to the elliptical chord with major diameter as longitudinal axis i.e Type2 joints are stronger than Type1 for all loading cases. • Failure for all the types starts near the weld joint and it happens on the chord and not on the weld itself. The reasonable agreement was obtained between the elastic analysis of ANSYS and LUSAS results for all types under all loading cases Reasonable agreement was obtained between the finite element analysis results and the experimental values for all loading cases. The Yield point's difference varies between 1.62 and 8.0 percent. This is well within the experimentation error limit of 10 %. for Tubular T-joint. Having validated the ANSYS package for elastic analysis of the Tubular T joint, it can be expanded to model and design the inclined brace joints like Y, K and X.

5. NOMENCLATURE

d = brace diameter l= length of brace K structural stiffness matrix,

D = chord diameter T=thickness of chord F global load vector $\beta = d/D$

L= length of chord t= thickness of brace Q global displacement vector

REFERENCES

1. Beale L.A and Toprac A.A. (1967), "Analysis of T.Y.K. welded connections," Bull structural steel committee, Texas
2. Chen.W. F. and Han. D. J., (1985), "Tubular Members in Offshore Structures", Pitman Advanced Publishing Program, Boston, MA
3. Chan .T and Wu .S (1985), "The Elastic Plastic finite element analysis of tubular joints of offshore drilling platform." Proceeding of International Conference on offshore structures, AMSTESDEM, pp. 813-821
4. Digre. K. A., Kreiger. W., Wisch. D. J., and Petrauskas.C, (1997), "API RP 2A Draft Section 17 Assessments of Existing Platforms," BOSS 94: Behavior of Offshore Structures, C. Hryssostomidis, Oxford, pp. 467–478
5. Jubran J.S and Cofer W.F. (1995)"Finite Element modeling of Tubular joints,"

Journal of structural engineering, Vol.129, pp. 496 –516.

6. Hamed A.F, Kalid Y.A.*and.Sahari A.Y and A.Y.Sahari.,(2001) "Finite Element and experimental analysis for the effect of elliptical chords shape on T-joints strength."Journal of Proceeding Mechanical Engineering, part E, proceeding of Institute of Mechanical Engineering. Vol. 215, pp. 123-131.
7. Kanatani H. (1986), "Experimental study on welded Tubular connections." Faculty of engineering report, Vol-12, pp.13-41, Kobe university, Japan.
8. Makino Y. and Kurobane Y. (1986). "Design of Tubular Joints," faculty of engineering report, Kumoto University, Japan, Vol.31, pp.1-28,.
9. Straub. D and Faber. M. H., 2005, "Risk Based Acceptance Criteria for Joints Subject to Fatigue Deterioration," ASME J. Offshore Mech. Arct. Eng., 127, 150–157.
10. Thandavamoorthy. T. S., 2009" Experimental and Numerical Investigations on Unstiffened Tubular T-Joints of Offshore Platforms" ASME J. Offshore Mech. Arct. Eng., Vol.131 / 041401-5.
11. UEG, 1985, "Design of Tubular Joints for Offshore Structures," Publication No. UR 33, Vol. 1, Vol. 2, Vol.3. Underwater Engineering Group, London.